ORIGINAL RESEARCH PAPER

Fuel Cells DOI: 10.1002/fuce.201000080

Synthesis and Properties of Random Copolymers of Functionalised Polybenzimidazoles for High Temperature Fuel Cells

J. A. Mader[1] and B. C. Benicewicz[1]*

[1] Department of Chemistry and Biochemistry and USC Nanocenter, University of South Carolina, 631 Sumter St., Columbia, SC 29208, USA

Received April 26, 2010; accepted November 02, 2010

Abstract

A series of polybenzimidazoles (PBIs) incorporating main chain sulphonic acid groups were synthesised as random copolymers with *p*-PBI in varying ratios using polyphosphoric acid (PPA) as both the polymerisation solvent and polycondensation reagent. The PPA process was used to produce high molecular weight phosphoric acid (PA) doped PBI gel membranes in a one-step procedure. These membranes exhibit excellent mechanical properties (0.528–2.51 MPa tensile stress and 130–300% tensile strain) even at high acid doping levels [20–40 mol PA/PRU (polymer repeat unit)] and high conductivities (0.148–0.291 S cm^{-1}) at elevated temperatures (>100 °C) with no external humidification, depending on copolymer composition. Fuel cell testing was conducted with hydrogen fuel and air or oxygen oxidants for all membrane compositions at temperatures greater than 100 °C without external feed gas humidification. Initial studies showed a maximum fuel performance of 0.675 V for the 25 mol% s-PBI/75 mol% *p*-PBI random copolymer at 180 °C and 0.2 A cm^{-2} with hydrogen and air, and 0.747 V for the same copolymer at 180 °C and 0.2 A cm^{-2} with hydrogen and oxygen.

Keywords: Fuel Cell, High Temperature Polymer Electrolyte Membrane, PPA Process, Random Copolymers of PBI, Sulphonated Polybenzimidazole

1 Introduction

Solid polymer electrolyte-based fuel cells have attracted much attention as a promising technology to meet today's growing energy needs [1]. Much research in the past has focused on perfluorosulphonic-acid (PFSA)-based polymers, such as Nafion®. This type of membrane relies on water for proton conduction, which limits the practical operating temperature to 80 °C and requires complicated water management systems. Due to these limitations, high temperature polymer membranes are of particular interest due to the advantages of faster electrode kinetics, high tolerance to fuel impurities, simplified system design and utilisation of waste heat [2]. The last 10 years has seen a great effort for the development of low cost, stable, hydrocarbon-based alternative membranes for both high and low temperature use. Typically, highly stable sulphonated aromatic polymers have been of interest for this application, but these membranes still rely heavily on water for proton conduction and show lower performance than the PFSA polymers. To overcome the lower temperature barrier imposed by a water dopant, much work has gone into developing membrane systems that can use alternative dopants, such as phosphoric acid (PA) or sulphuric acid and has been recently reviewed [3].

PA-doped polybenzimidazole (PBI)-based polymers have emerged as the most promising candidate for high temperature (120–180 °C) fuel cell membranes. PA-doped poly(2,2'-(1,3-phenylene)-5,5'-bibenzimidazole), or *m*-PBI, was first introduced as a membrane candidate in the early 1990's by

[*] *Corresponding author, benice@sc.edu*

Wainright et al. [4]. These polymers show high ionic conductivities at elevated temperatures, low gas permeability, excellent thermochemical stability and nearly zero water drag coefficient [4–6]. Research has typically focused on the *m*-PBI or AB-PBI structures due to commercial availability of polymers and monomers and ease of film casting from organic solvents. After casting from organic solvents, a film can be placed into an acid bath to become doped with PA. A wide variety of doping levels (3–16 mol PA/PRU) and conductivities (10^{-5}–0.13 S cm^{-1}) have been reported in recent years [4, 7–10], and tend to be dependent on both casting solvent and doping process. Typically, the membrane mechanical properties become weaker with increased doping levels, limiting practical operating values to 6–10 moles PA per mole PRU (mol PA/PRU).

In order to improve properties such as mechanical strength, doping levels, conductivity and stability, blends or copolymers of *m*-PBI with various sulphonated hydrocarbon-based polymers such as sulphonated polysulphone, sulphonated poly(ether ether ketone), sulphonated polystyrene and sulphonated poly(phenylquinoxalines) have been synthesised and characterised [11–26], but little fuel cell performance data has been published to date. Additionally, much of the characterisation of these polymers has been performed for low temperature water-based applications, and not high temperature PA-based systems.

A new method has been developed recently to produce highly doped PBI films via a one-step synthesis [27–32]. The polyphosphoric acid process (PPA process) can be used to synthesise a wide variety of PBI chemistries and removes the time intensive, multi-step process needed to produce conventional PA-doped PBI films. A number of homopolymers and copolymers have been investigated using the PPA process, including *m*-PBI, AB-PBI, *p*-PBI [32], pyridine-based PBIs [28], dihydroxy-PBI [29] and fluorinated PBIs [30, 31].

Many types of copolymers are attainable via step-growth polymerisation. It has been well documented in the literature that polymer architecture affects polymer properties. The work in this paper focuses combining the chemistries of low temperature membranes (sulphonated hydrocarbons) with the high temperature, acid-based properties of PBI membranes. Based on the promise of the recently developed s-PBI homopolymer [33], the synthesis and characterisation of random copolymers of s-PBI and *p*-PBI (Scheme 1) is of great interest. The *p*-PBI polymer was chosen due to its excellent mechanical properties, high acid doping levels and stability in a high temperature acidic environment. Random copolymers were developed and characterised in terms of their chemical structure, polymer and membrane properties and high temperature (120–180 °C) acid-based fuel cell performance.

2 Experimental

2.1 Materials

The monosodium salt of 2-sulphoterephthalic acid (s-TPA, 98%) was purchased from TCI America and dried in a vacuum oven overnight at 120 °C before use. Terephthalic acid (TPA, 99+%) was purchased from Amoco and used as supplied, while 3,3′,4,4′-tetraaminobiphenyl (TAB, polymerisation grade) was donated by Celanese Ventures, GmbH and used as received. PPA (115%) was used as supplied from Aldrich Chemical Co. or FMC Corporation. PA (85%) was used as supplied from Fisher Scientific.

2.2 Synthesis of Random Copolymers

The s-PBI/*p*-PBI random copolymers were synthesised using the following general procedure and are depicted in Scheme 1: TAB (2.889 g, 13.48 mmol), TPA (1.120 g, 6.74 mmol) and 2-sulfoterephthalic acid, monosodium salt (s-TPA, 1.808 g, 6.74 mmol) were added to a 100 mL three neck resin reaction flask in a nitrogen atmosphere glovebox, followed by the addition of 100–120 g of PPA (3–3.6 wt.-% polymer solids). The mixture was stirred by an overhead mechanical stirrer under a slow nitrogen purge. The reaction temperature was controlled by a programmable temperature controller with ramp (increasing to a specified temperature over a specified time period) and soak (maintaining the specified temperature for the specified time) capabilities and the profile is described below.

Temperature profile:

- 120 °C ramp: 2 h, soak: 2 h.
- 140 °C ramp: 2 h, soak: 3.5 h.
- 170 °C ramp: 1 h, soak: 3 h.
- 195 C ramp: 1 h, soak: 10–13 h.

The final reaction conditions were changed slightly to optimise the polymerisation temperatures and conditions for both s-PBI and *p*-PBI type polymers, depending on copolymer ratios. The TPA/s-TPA ratios were changed as necessary to make copolymers with varying s-PBI compositions (x = 25,

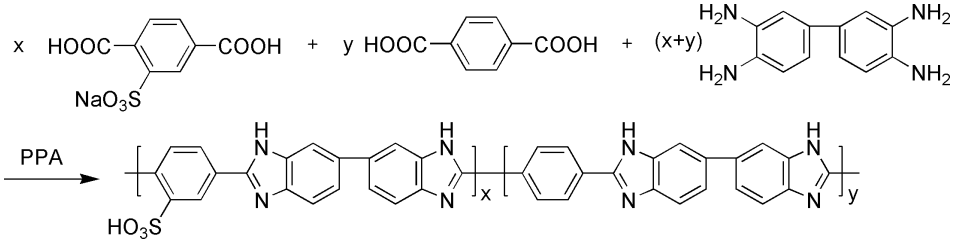

Scheme 1 Synthesis of s-PBI/*p*-PBI random copolymers via the PPA process.

50 or 75 mol%). As the reaction proceeded, the mixture became brown or green and increased in viscosity. A small amount of the reaction mixture was isolated in water, pulverised, neutralised with concentrated ammonium hydroxide, washed with distilled water to neutrality and dried under vacuum for 24 h at 120 °C to obtain a dry copolymer sample for characterisation.

2.3 Film Formation

After polymerisation, the reaction temperature was raised to 220 °C to lower solution viscosity for casting. Random copolymer films were prepared by direct casting of the hot polymerisation solution onto clean glass plates using a Gardner doctor blade at thicknesses of 5–15 mils (127–381 µm). The final solution viscosity and solids content was adjusted using 85% PA during the 220 °C portion of the polymerisation, if necessary. The final casting solids concentration was 3.0 wt.-% for the 25/75 and 50/50 s/*p*-PBI random copolymers and 3.6 wt.-% for the 75/25 s/*p*-PBI random copolymer. After casting, the films were placed in a controlled humidity chamber (55 ± 5%) for 24 h to hydrolyse PPA to PA, inducing a sol–gel transition to produce a PA-doped gel membrane.

2.4 Characterisation Techniques

To measure the inherent viscosity (IV), the neutral, dried polymer isolated from water was dissolved in concentrated sulphuric acid (96%) at a concentration of 0.2 dL g^{-1}. The IV was measured in a Canon Ubbelhode viscometer at 30 °C. PA content was determined by titrating a membrane sample with standard 0.1 N sodium hydroxide solution with a Metrohm® 716 DMS Titrino titrator. The samples were washed with water and dried under vacuum at 120 °C overnight to obtain the dry polymer weight for calculation of the PA doping level. The doping level, *X*, reported as moles of PA per mole of PRU (mol PA/PRU), was calculated from Eq. (1):

$$\text{PA doping level } X = \frac{V_{\text{NaOH}} \cdot C_{\text{NaOH}}}{W_{\text{dry}}/M_{\text{w}}} \quad (1)$$

where V_{NaOH} and C_{NaOH} are the volume and normal concentration of the sodium hydroxide titer, W_{dry} the dry polymer sample weight and M_{w} is the average molecular weight of the random copolymer based on molar ratios. The ionic conductivity of the membranes was measured using four-probe AC impedance spectroscopy with a Zahner IM6e spectrometer in the frequency range of 1 Hz to 100 KHz. A two-component model with a resistor in parallel with a capacitor was used to fit the experimental data of membrane resistance across the frequency range. The proton conductivity was calculated from room temperature to 180 °C using Eq. (2):

$$\sigma = \frac{D}{LWR} \quad (2)$$

where *D* is the distance between the two current electrodes, *L* and *W* are the thickness and width, respectively, and *R* is the measured resistance value. The distance between the sensor and test electrodes was 2.0 cm. The membrane mechanical properties were measured in atmospheric conditions using an Instron Model 5846 system with a 100 N load cell. The crosshead speed was 10 mm min^{-1} and samples were preloaded to 0.1 N. The dumb-bell shaped specimens were cut according to ASTM standard D683 (Type V specimens). Thermogravimetric analysis (TGA) of dried polymer samples was conducted using a TA Instruments Q5000 with nitrogen or air flow rates of 25 mL min^{-1} and heating rate of 10 °C min^{-1}. TGA was performed from room temperature to 700 °C. Attenuated total reflectance (ATR) Fourier transform infrared spectroscopy was performed using a Perkin-Elmer Spectrum 100 Fourier transform-infrared spectrometer with three-reflection diamond/ZnSe crystal. Spectroscopy was performed on dried polymer powders in the range of 4,000–650 cm^{-1}.

Fuel cell performance of the random copolymers was measured using 50 cm^2 single cells (active area: 45.15 cm^2). The membrane electrode assembly (MEA) was prepared by hot pressing an electrode:membrane:electrode sandwich (4.45 MPa) for 30 s at 140 °C. Electrodes were received from BASF Fuel Cell, Inc. with 1 mg cm^{-2} Pt catalyst loading at the anode and 1 mg cm^{-2} Pt alloy (0.7 mg cm^{-2} Pt) at the cathode, and were used without additional manipulation (e.g. addition of PA to the electrode). Polarisation curves were obtained from 120 to 180 °C with non-humidified hydrogen fuels and air or oxygen oxidant at stoichiometries of 1.2 and 2.0, respectively, and ambient pressure.

3 Results and Discussion

3.1 Synthesis and Characterisation of s-PBI/p-PBI Random Copolymers

To form random copolymers of s-PBI and *p*-PBI, the s-TPA and TPA monomers were added in the desired ratios to the appropriate amount of TAB under a nitrogen atmosphere. PPA was then added to the monomers as the polymerisation solvent. High molecular weight polymers (IV's > 1.0 dL g^{-1}) were formed during the initial attempt and the synthetic parameters were used for further polymerisations. The final solids concentration of 3 wt.-% was chosen for the 25/75 and 50/50 s-PBI/*p*-PBI random copolymers due to the high *p*-PBI content. The typical final solids concentration for the *p*-PBI homopolymer is 2.5 wt.-% because high polymerisation solution viscosities resulted from higher solids content, leading to casting difficulties. The final solids concentration of the s-PBI homopolymer was generally 3.5–4 wt.-%, where the optimal balance of desired fuel cell membrane properties was achieved. For these reasons, the higher s-PBI content 75/25 s-PBI/*p*-PBI random copolymer was synthesised with a higher final solids concentration of 3.6 wt.-%. The random copolymer properties are reported in Table 1, and the acid loading,

Table 1 s-PBI/*p*-PBI random copolymer polymerisation and characterisation results for polymers and PA-doped membranes before fuel cell fabrication and testing.

Sample ID	Membrane type	Solids content[a]	IV[b]	PA[c]	Conductivity / S cm^{-1}[d]	Thickness / mil (μm)	TS / MPa[e]	Tensile Strain /%
1a	75/25 s-PBI/*p*-PBI	3.60	1.91	20.32	0.157	3.58 (90.9)	0.834	136
1b	75/25 s-PBI/*p*-PBI	3.60	1.91	29.12	0.157	14.37 (365)	2.51	154
2a	50/50 s-PBI/*p*-PBI	3.0	2.24	33.07	0.148	5.25 (133)	1.12	256
2b	50/50 s-PBI/*p*-PBI	3.0	2.24	28.49	0.148	2.86 (72.6)	0.583	220
3	25/75 s-PBI/*p*-PBI	2.90	3.29	40.69	0.291	4.09 (104)	0.876	285
4	s-PBI	3.42	1.86	39.95	0.194	15.28 (388)	1.56	160

(a) Casting solids content: wt.-%.
(b) IV: Measured at 30 °C in concentrated sulphuric acid: dL g^{-1}.
(c) PA doping levels: mol PA/PRU.
(d) Conductivity measured at 180 °C.
(e) TS, tensile stress at break.

conductivity and mechanical properties are discussed in later sections.

The relationship between s-PBI content and IV is shown in Figure 1. There was a decrease in random copolymer IV with increased s-PBI content, and the values fall between those of the two homopolymers. The lowering of the IV with increasing s-PBI content is due to the lower initial IV's of the s-PBI homopolymer (typically ~1.2 dL g^{-1}). All the polymerisations indicate the formation of high molecular weight polymer (IV > 1.0 dL g^{-1}), which allows for the formation of mechanically robust gel films. More detailed polymer molecular weight characterisation was precluded by the insolubility of the polymers in common organic solvents. The change in IV values is at least partially attributed to the changes in the Mark-Houwink coefficients used to relate polymer molecular weight and IV values, with changes in the chemical composition of the copolymers.

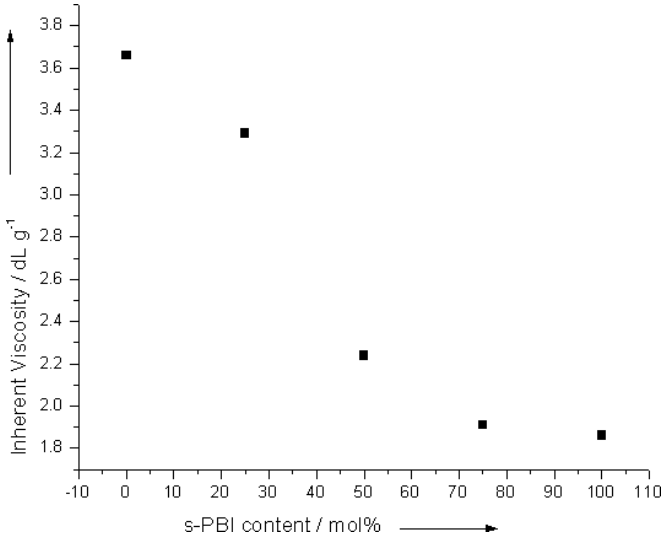

Fig. 1 IV trends with increasing s-PBI content in the random copolymer.

The characterisation of polymer structure and stability was performed using infrared spectroscopy and TGA. NMR and elemental analysis of these polymers was attempted, but the obtained data were not meaningful. PBIs prepared with *para*-oriented phenyl rings (rather than the typical *meta*-orientation) are extremely insoluble in typical organic solvents for these systems (e.g. dimethylacetamide), making NMR characterisation extremely difficult. Indeed, concentrated sulphuric acid was the only solvent found to dissolve these polymers at low concentrations, and the corresponding NMR spectra were unclear and interpretation was not possible. Historically, many papers have reported that the high thermal stability of wholly aromatic PBIs, even at extremely high temperatures in air, makes it difficult to get accurate element analysis results. Triple pass ATR Fourier transform infrared spectroscopy was used to confirm the incorporation of the s-PBI into the copolymer structure. The spectra of *p*-PBI and the random copolymers are shown in Figure 2. The peak at 800 cm^{-1} corresponds to the symmetric S-O stretch, while the bands at 1,022 and 1,070 cm^{-1} are due to the symmetric S-O stretches. The strong bands at 1,168 and 1,223 cm^{-1} are due to asymmetric S-O stretching. The peak at 1,629 cm^{-1} is indicative of the C-C/C-N stretches in the imidazole ring. The absence of a band in the 1,650–1,780 cm^{-1} region indicates complete closure of the imidazole ring. The SO peaks are in agreement with the literature for sulphonated PBIs [34–36], and are not present in the unfunctionalised *p*-PBI spectrum.

TGA was performed to determine the stability of the random copolymers at fuel cell operating temperatures (120–180 °C), as seen in Figure 3a. The sulphonic acid group begins decomposition at ~425 °C for all random copolymers, consistent with the s-PBI homopolymer produced via the PPA process and the literature for sulphonated hydrocarbon polymers [23, 35–43]. The *p*-PBI curve does not show a large weight loss at this temperature, confirming that the weight loss in this temperature range is due to the sulphonic acid moiety. Figure 3b shows a representative example of the 50/50 s-PBI/*p*-PBI polymer in both nitrogen and air. Significant decomposition is not seen until ~425 °C, where the sulphonic acid group decomposes, as in nitrogen. The vast majority of polymer decomposition occurs above 500 °C in air, but total decomposition is not observed, even at 700 °C. The initial sulphonic acid group decomposition temperature is significantly above the desired fuel cell operating temperatures, and excellent polymer stability is observed up to 200 °C in both nitrogen and air. The small weight losses below this temperature for all polymers are attributed to absorbed water due to the hygroscopic nature of PBI-type polymers.

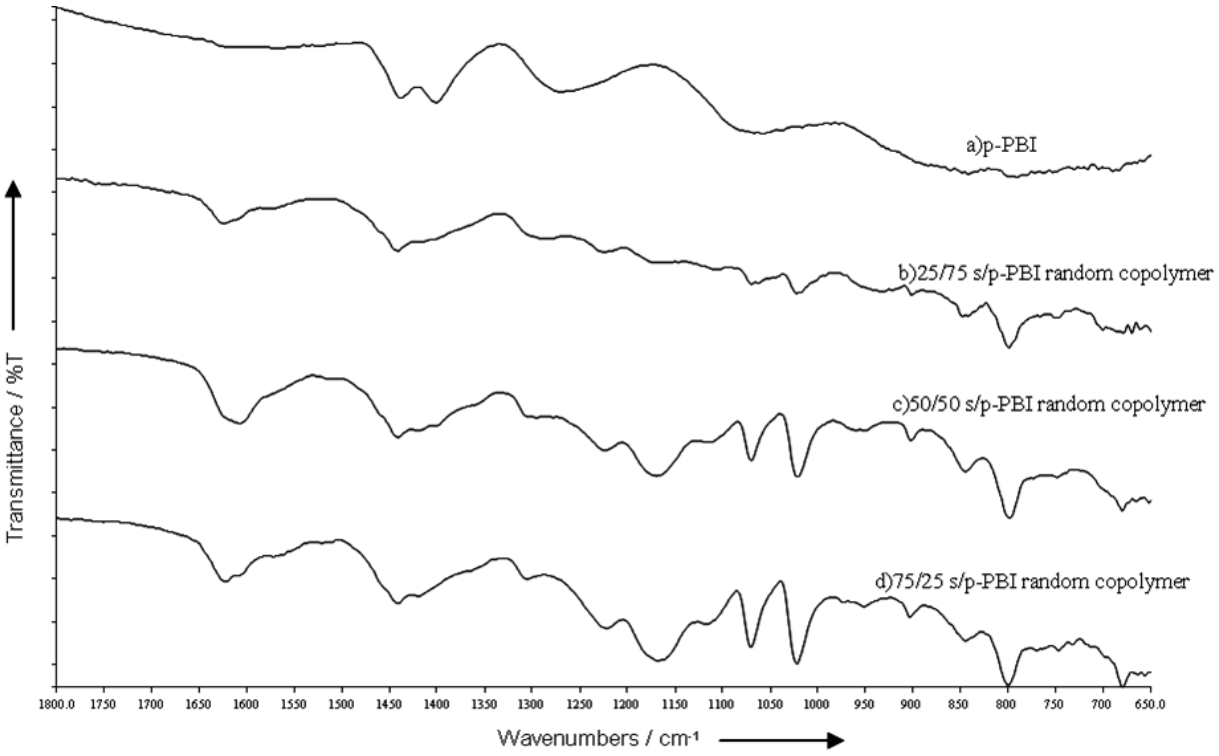

Fig. 2 ATR triple pass infrared spectra of (a) *p*-PBI; (b) 25/75 s-PBI/*p*-PBI random copolymer; (c) 50/50 s-PBI/*p*-PBI random copolymer; and (d) 75/25 s-PBI/*p*-PBI random copolymer.

The sample weight loss in the sulphonic acid group decomposition temperature range (425–525 °C) increases linearly with increasing s-PBI content in the copolymer (Figure 3a inset). Thus, the lowest weight loss was seen for the 25/75 s-PBI/*p*-PBI random copolymer (4.09 wt.-%), while the highest was seen for the 75/25 s/*p*-PBI random copolymer (12.5 wt.-%). The weight loss of just the sulphonic acid moiety was also investigated across the various compositions to see if the random copolymer structure and morphology affected the stability of the functional group. The overall sulphonic acid group loss remained consistent around ~16–17 wt.-% of the total sulphonic acid group content, with a slightly higher loss for the 50/50 s-PBI/*p*-PBI random copolymer. The sulphonic acid group comprised 20.91 wt.-% of the s-PBI PRU, indicating the desulphonation step was not complete over this temperature range or resulted in a derivative structure that still retained sulphur content.

3.2 Film Formation

One of the largest barriers to commercialisation of the more robust *p*-PBI-based polymers has been its insolubility in typical organic solvents. By direct polymerisation of the desired monomers in PPA, followed by immediate film casting, this limitation has been overcome. Acid-doped films of both s-PBI and *p*-PBI homopolymers have been produced previously by the PPA process [29, 33]. Gel films of the random copolymers were successfully prepared via a one-pot synthesis and casting using the PPA process. The polymerisations produced high molecular weight (IV > 1.0 dL g^{-1}) random copolymer membranes with controlled s-PBI/*p*-PBI ratios. If necessary, the final solution viscosity was adjusted using 85% PA. Typically, the higher the *p*-PBI content in the copolymer, the greater the viscosity and subsequent molecular weights. All compositions formed red–orange translucent gel films under appropriate polymerisation and hydrolysis conditions. Films were typically cast at 5–10 mils (127–254 μm) using a Gardner doctor blade and placed in a humidity chamber at relative humidity (RH) of 55 ± 5% for 24 h. Absorption of water by PBI and PPA allowed an *in situ* hydrolysis of PPA to PA which induced a sol–gel transition to yield highly acid-doped gel membranes. For all random copolymer compositions, the gel state remained stable at fuel cell operating temperatures (120–180 °C).

3.3 Membrane Properties

3.3.1 Membrane Doping Levels and Proton Conductivity

The acid doping levels (mol PA/PRU) of the random copolymer films cast from PPA solutions were determined by titration with 0.1 N sodium hydroxide solution. The average molecular weight of the repeat unit was used for the PA loading calculations. The polymer characterisation results are reported in Table 1. For batches 1 and 2, the membrane thickness of two different random copolymer compositions was varied to determine if there were large differences in properties with membrane thickness. The two 75/25 s-PBI/*p*-PBI

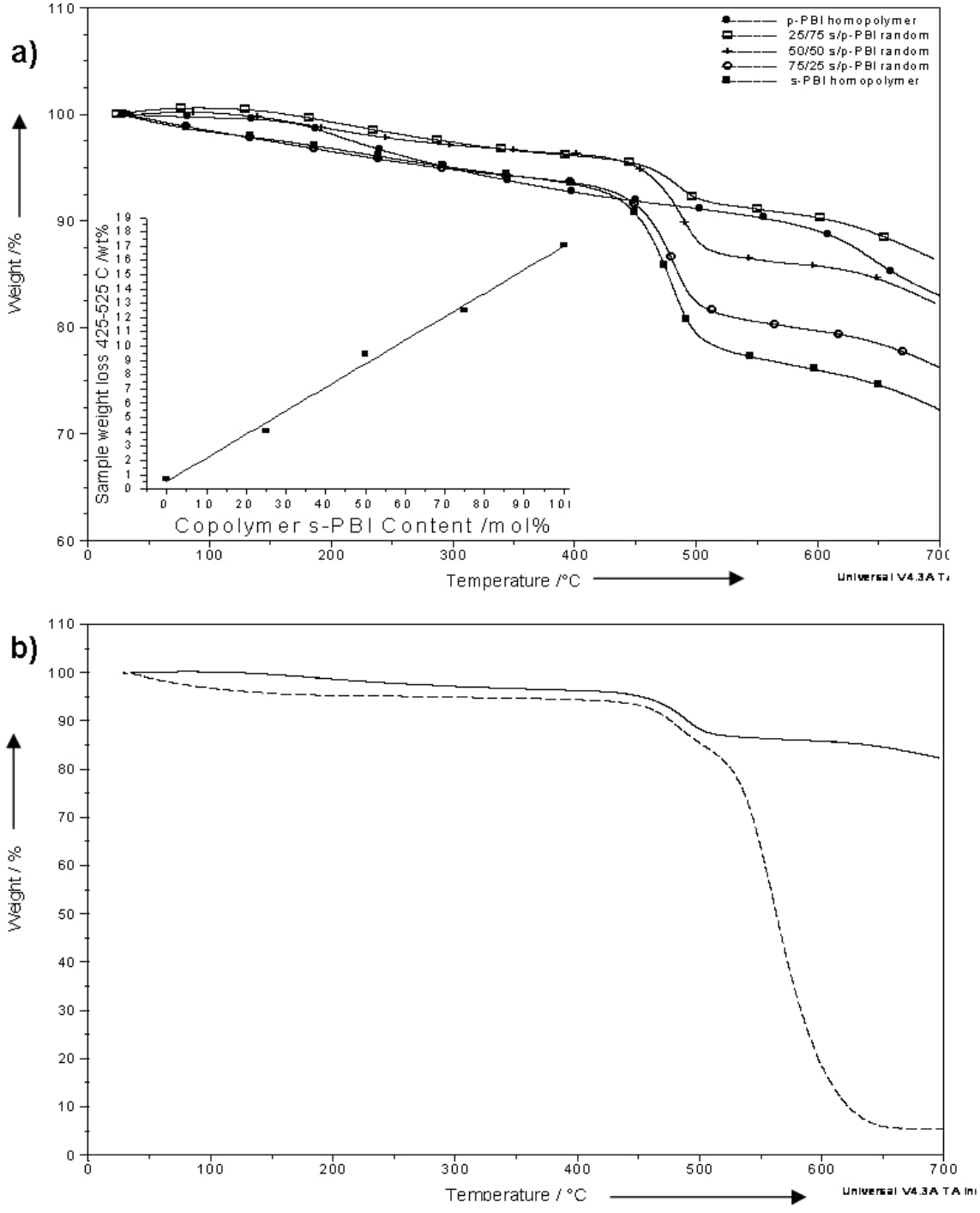

Fig. 3 TGA curves (a) in nitrogen of *p*-PBI homopolymer (circles), 25/75 s-PBI/*p*-PBI random copolymer (open squares), 50/50 s-PBI/*p*-PBI random copolymer (crosses), 75/25 s-PBI/*p*-PBI random copolymer (open circles) and s-PBI homopolymer (closed squares), Inset: Sample weight loss from 425 to 525 °C compared to s-PBI content in the random copolymer; and (b) representative comparison of the 50/50 s-PBI/*p*-PBI random copolymer in nitrogen (solid line) and air (dashed line)

random copolymers were cast from the same polymer solution, but with different gate thicknesses on the doctor blade and the property differences are discussed in the Section 3.3.2. The 50/50 s-PBI/*p*-PBI random copolymers were cast from the same batch of polymer solution at different gate thicknesses. The random copolymer membranes were doped with 20–40 mol PA/PRU, based on composition. The lowest loading (20.32 mol PA/PRU) was seen for the 75/25 s-PBI/*p*-PBI random copolymer, while the 50/50 s/*p*-PBI copolymer retained 33.07 mol PA/PRU. The 25/75 s/*p*-PBI random copolymer had a doping level of 40.69 mol PA/PRU. The PA content increased nearly linearly with decreasing s-PBI con-

tent, indicating a stronger interaction between PA and *p*-PBI than between PA and s-PBI. The doping levels found were similar to the s-PBI homopolymer (22–55 mol PA/PRU), and are significantly higher than those values reported in the literature for conventionally prepared PBI and copolymer membranes.

Table 2 Effect of fuel cell operating temperature and oxidant gas composition on s-PBI/*p*-PBI random copolymers with respect to voltage (*V*) at 0.2 A cm^{-2}.

	50/50 s-PBI/*p*-PBI random copolymer			25/75 s-PBI/*p*-PBI random copolymer		
Temp. / °C	Air	O_2	ΔV / mV	Air	O_2	ΔV / mV
180	0.6296	0.6997	70.1	0.6753	0.7465	71.2
160	0.5990	0.7022	103.2	0.6633	0.7358	72.5
140	0.5929	0.6909	98.0	0.6449	0.7218	76.9
120	0.5753	–	–	0.6202	0.7065	86.3

All compositions of the random copolymers exhibited high proton conductivity at high temperatures and remained mechanically intact during measurement. The conductivity results are shown in Figure 4. The conductivities of the 75/25, 50/50 and 25/75 s-PBI/*p*-PBI at 180 °C are 0.157, 0.148 and 0.291 S cm^{-1}, respectively. The higher value of the 25/75 s-PBI/*p*-PBI is likely due to the higher acid loading level and is slightly higher than the s-PBI homopolymer with a similar acid doping level (44 mol PA/PRU, 0.254 S cm^{-1}) and also the *p*-PBI homopolymer (62 mol PA/PRU, 0.276 S cm^{-1}). The conductivities of the 50/50 and 75/25 s-PBI/*p*-PBI random copolymers are comparable to or higher than the s-PBI homopolymer at similar acid loading levels (28 mol PA/PRU, 0.161 S cm^{-1}) and were significantly improved over values previously reported in the literature (10^{-6}–10^{-1} S cm^{-1} [8, 20, 23, 26, 34–39, 42–45] for sulphonated hydrocarbon-based polymers. As can be seen in Figure 4 and Table 1, the conductivity of the 25/75 s-PBI/*p*-PBI random copolymer is significantly higher than the other copolymer compositions. It is known that gel morphologies allow the incorporation of high volumes of liquid and that random copolymer morphologies may have improved properties over either homopolymer. In this case, the morphology of the polymers produced via the PPA process retains large amounts of PA. Because the conductivity of the random copolymers increased with higher doping levels, we must preliminarily conclude that the random copolymer morphology contributed to the increased conductivity. A total of three polymerisation and film casting runs yielded the same trend in conductivity, with the 25/75 s-PBI/*p*-PBI conductivity being markedly higher than the other compositions.

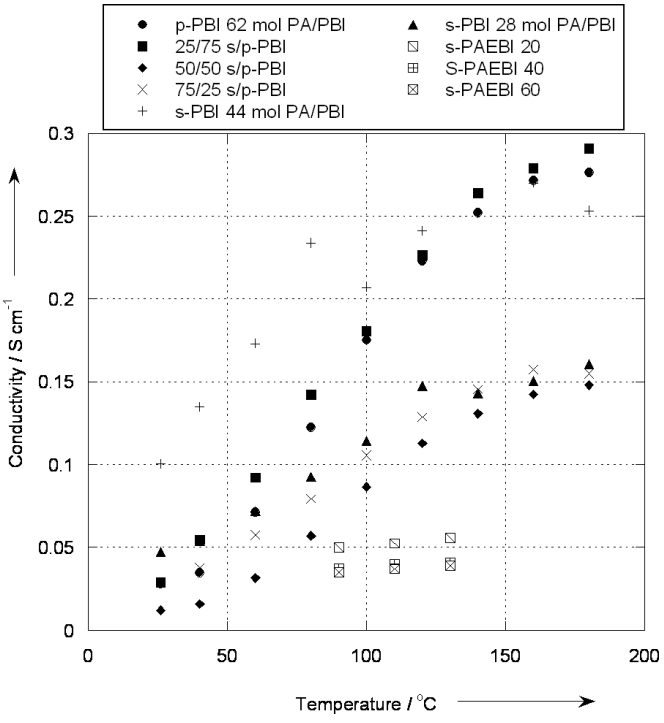

Fig. 4 Conductivity *vs.* temperature for PPA process s-PBI (crosses and closed triangles), *p*-PBI (circles), 25/75 s-PBI/*p*-PBI random copolymer (closed squares), 50/50 s-PBI/*p*-PBI random copolymer (closed diamonds), 75/25 s-PBI/*p*-PBI random copolymer (*x* marks) and literature [15] s-PAEBI random copolymers with varying degrees of sulphonation (20, 40 and 60 mol%).

Jeong et al. [14] developed a PA-doped sulphonated poly(-aryl ether benzimidazole) (s-PAEBI) random copolymer system with controlled degree of sulphonation. The doping levels were dependent on PA bath concentration and degree of sulphonation in the polymer and were between 2.5 and 5% for membranes with 20–60% sulphonation. Non-humidified conductivities of membranes doped in 10 M PA were temperature and composition dependent and ranged from ~3.5 × 10^{-2} to ~5.6 × 10^{-2}S cm^{-1} (90–130 °C, 20–60% sulphonation), and are also shown in Figure 4. In comparison to these values, the s-PBI/*p*-PBI random copolymers developed in this work had significantly higher conductivities by five to ten times, and at least four times the acid loading levels.

3.3.2 *Mechanical Properties*

The mechanical properties of the random copolymers were investigated to determine composition and thickness effects. It was found that the incorporation of *p*-PBI into the random copolymer improved the mechanical properties over the s-PBI homopolymer (avg: 0.804 MPa tensile stress at break, 69.64% tensile strain at break). The 75/25 s-PBI/*p*-PBI random copolymer was tested for mechanical properties at two different thicknesses. It was found that a 3.58 mil (90.9 µm) thick membrane exhibited a tensile stress at break of 0.834 MPa and tensile strain of 136%. The same copolymer composition with a 14.4 mil (365 µm) thickness showed properties of 2.508 MPa and 154% for tensile stress and strain, respectively, and these properties were improved over the *p*-PBI homopolymer. Thin films are more susceptible to defects, and this effect is likely exacerbated by the low polymer solids in the gel films, especially considering these are hand-cast films.

The 50/50 s-PBI/p-PBI random copolymer also showed thickness dependent properties. A 2.86 mil (72.7 µm) thick-

ness membrane showed a tensile stress and strain at break of 0.583 MPa and 220%, respectively, while a 5.25 mil (133 µm) thickness membrane exhibited 1.124 MPa and 256% tensile stress and strain, respectively. Two sets of the 25/75 s-PBI/*p*-PBI random copolymer with different IV's were tested. The membrane with an IV of 2.32 dL g^{-1} and thickness of 3.68 mil (93.5 µm) showed tensile stress of 0.714 MPa and tensile strain of 321%, while the membrane with an IV of 3.29 dL g^{-1} and thickness of 4.09 mil (104 µm) showed tensile stress and strain of 0.876 MPa and 285%, respectively. The higher MW of the second sample is likely the reason for the increase in tensile stress. The tensile stress and modulus increased with membrane thickness (within the same composition). The tensile stress remained approximately the same across the different compositions of membrane with the same thicknesses. The tensile strain of the 25/75 and 50/50 s-PBI/*p*-PBI random copolymers was improved over the s-PBI and *p*-PBI homopolymers at all thickness tested. The 75/25 s-PBI/*p*-PBI random copolymer had lower tensile strain at break than the homopolymers, but exhibited higher modulus and tensile stress at break. The homopolymers had higher tensile stress and strain at break than the 50/50 and 25/75 s-PBI/*p*-PBI random copolymers. In general, tensile strain increased with decreasing sulphonated composition and greater thickness. This was expected based on the random copolymer morphology, where final polymer properties are typically an average of the two-homopolymer systems. All membranes were able to undergo MEA fabrication and fuel cell testing, even for lower thicknesses, indicating the mechanical stability of the random copolymers.

3.4 Fuel Cell Performance

Figure 5 shows the detailed fuel cell performance for the s-PBI/*p*-PBI random copolymers with hydrogen and different oxidants. The highest performance was observed for the 25/75 s-PBI/*p*-PBI random copolymer. The 50/50 s-PBI/*p*-PBI had the next highest performance (except at 160 °C), followed by the 75/25 s-PBI/*p*-PBI polymer. The addition of even a small amount of *p*-PBI (25 mol%) into the random copolymer improved performance, and as the amount of *p*-PBI in the copolymer increased, so did the fuel cell performance, as seen in Figure 6. The 25/75 s-PBI/*p*-PBI random copolymer (41 mol PA/PRU) had improved performance over the PPA process s-PBI membrane with low acid loading level (30 mol PA/PRU). Additionally, the 25/75 s-PBI/*p*-PBI random copolymer displayed comparable or better performance than the PPA process s-PBI membrane with high acid loading (52 mol PA/PRU), even though the acid loading of the random copolymer was lower (41 mol PA/PRU), suggesting the copolymer structure/morphology contributed to the improvements. The 50/50 and 75/25 s-PBI/*p*-PBI random copolymers showed lower performance than both s-PBI membranes at all temperatures, likely due to the similar or lower acid loading levels and lower conductivities in comparison to the homopolymer. All random copolymers showed lower

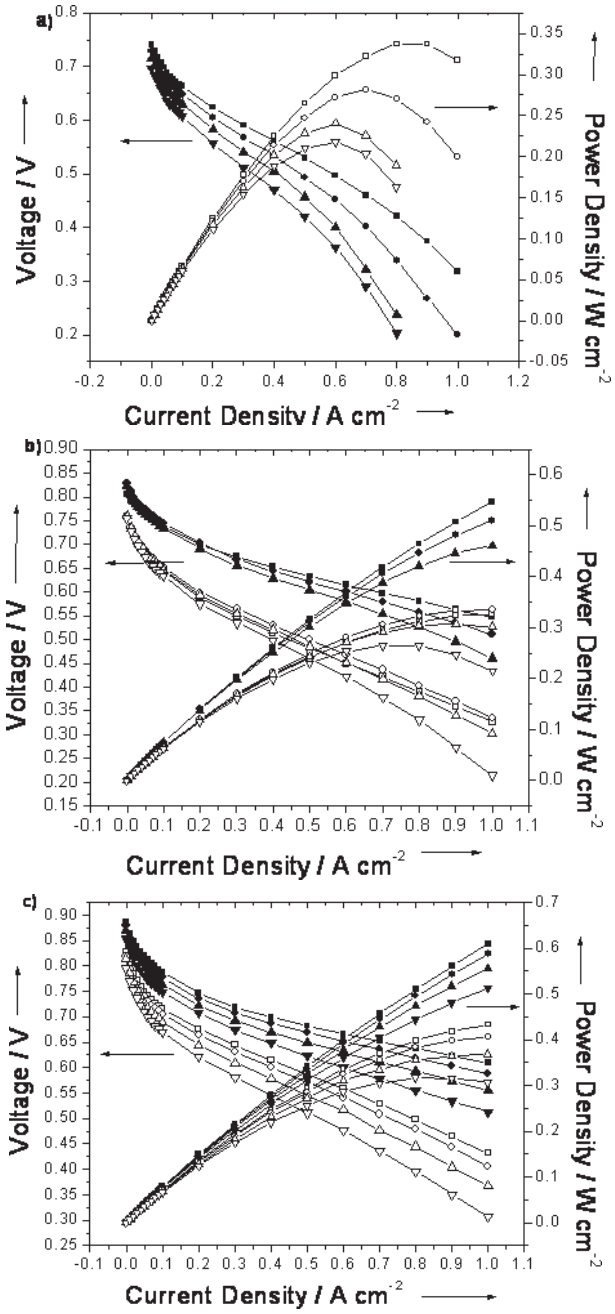

Fig. 5 Fuel cell performance of (a) 75/25 s-PBI/*p*-PBI random copolymer with hydrogen and air: polarisation curves (filled symbols) and power density curves (open symbols); (b) 50/50 s-PBI/*p*-PBI random copolymer polarisation curves and power density curves with hydrogen and air (open symbols) or oxygen (filled symbols); and (c) 25/75 s-PBI/*p*-PBI random copolymer polarisation curves and power density curves with hydrogen and air (open symbols) or oxygen (filled symbols). Squares: 180 °C, diamonds: 160 °C, triangles: 140 °C and upside down triangles: 120 °C.

performance than the *p*-PBI homopolymer (IV = 3.42 dL g^{-1}, 32.28 mol PA/PRU, 0.344 S cm^{-1}) tested under the same fuel cell conditions, likely due to the lower conductivity of the random copolymers.

Performance increased greatly for all membrane compositions tested with oxygen as the oxidant gas compared to air.

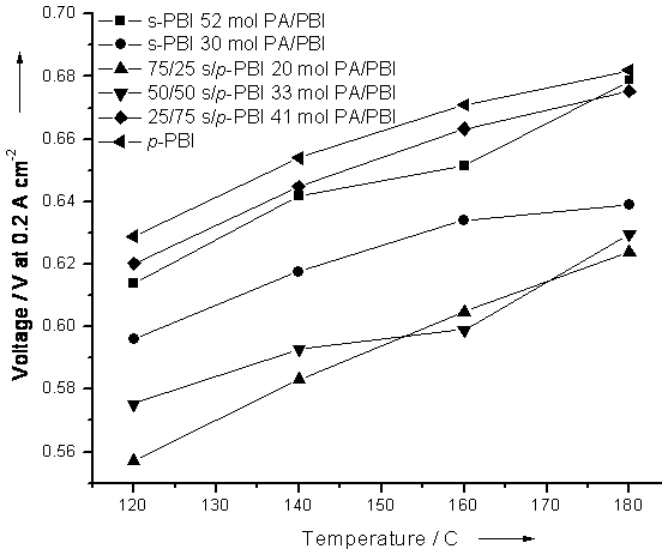

Fig. 6 Comparison of hydrogen/air performance of s-PBI (52 mol PA/PRU, squares; 30 mol PA/PRU, circles), 75/25 s/*p*-PBI random copolymer (triangles), 50/50 s/*p*-PBI random copolymer (upside down triangles), 25/75 s/*p*-PBI random copolymer (diamonds) and *p*-PBI homopolymer (left-pointing triangles) at different temperatures at 0.2 A cm^{-2}.

The calculated improvement when switching from air to oxygen is ~65 mV, according to the Nernst Equation. The increases observed for the random copolymers were composition and temperature dependent and range from ~70 to 103 mV. The differences are more extreme at lower temperatures and higher s-PBI content, as seen in Table 2. The larger than theoretical increases may have been due to the longer break in times when collecting polarisation curve data and also to overcoming mass transport limitations experienced with air, but the increases were clearly not related solely to the differences in oxygen partial pressure. It is likely that the unoptimised pressing conditions may have allowed overcompression of the membrane, forcing some polymer into the electrode layer. The polymer in the electrode layer coated the platinum catalyst, rendering it inaccessible to the oxidant and lead to starvation at higher current densities. As the concentration of oxygen increased when switched from air, more gas was able to diffuse through the polymer and reach the catalyst, improving the performance.

To date, there is little fuel cell performance data in the literature for PBI-based random copolymers or blends. Kim et al. [46] prepared random copolymers of *m*-PBI and sulphonated *m*-PBI prepared with 5-isophthalic acid. The polymer had a doping level of 400% and showed hydrogen–air fuel cell performance of ~0.64 V at 0.2 A cm^{-2} at 150 °C. However, fuel cell size, gas stoichiometries and pressures and Pt catalyst loading were not specified, making valid comparisons difficult. These data were higher than the 75/25 and 50/50 s-PBI/*p*-PBI random copolymers, but significantly lower than the 25/75 s-PBI/*p*-PBI random copolymer, and is the only report of acid-doped PBI random copolymer fuel cell data in the literature. The reported data in the literature was for m-PBI/sulphonated hydrocarbon polymers with different structures and doping levels than the novel polymers presented in this work, and thus, valid comparisons are not possible.

4 Conclusions

A series of novel high molecular weight random copolymer gel membranes with controlled ratios of s-PBI and *p*-PBI were successfully prepared using PPA as the polycondensation and casting solvent. TGA and ATR-FTIR confirmed the presence of the sulphonic acid moiety in the polymer structure and indicated that the incorporated sulphonic acid groups were stable under fuel cell operating temperatures, even in air at elevated temperatures (Figure 3b). It was found that the molecular weights, acid doping levels, proton conductivities and mechanical properties were comparable to or improved over the s-PBI homopolymer, depending on the copolymer composition. In general, polymer properties were an average of the two-homopolymer systems. The acid loading of the random copolymers was composition dependent, with higher s-PBI content leading to lower acid doping levels (20–40 mol PA/PRU, 75–25 mol% s-PBI). Conductivity values increased with decreasing s-PBI content, which is likely a function of the increased acid-doping level. The 25/75 s-PBI/*p*-PBI random copolymer showed improved conductivity values over both homopolymers, while the other random copolymer compositions exhibited lower or comparable performance to the s-PBI homopolymer with low acid doping (28 mol PA/PRU) and lower conductivities compared to *p*-PBI. In summary, different copolymer compositions showed different levels of PA in the membranes and higher acid doping levels led to higher proton conductivities, even when the PA doping levels were all above 20 mol PA/PRU. All random copolymer compositions were significantly improved over the s-PAEBI membranes produced in the literature with 20–60% sulphonation and doped in 10 M PA. Incorporating even a small amount of *p*-PBI (25 mol%) into the random copolymer increased membrane mechanical properties and fuel cell performance among the random copolymer compositions for both hydrogen–air and hydrogen–oxygen. All random copolymers showed excellent fuel cell performance with both hydrogen–air and hydrogen–oxygen. The 25/75 s-PBI/*p*-PBI random copolymer showed higher fuel cell performance than the s-PBI polymer with low acid loading, and better or comparable performance to the s-PBI polymer with high acid loading, depending on temperature. The membrane properties and fuel cell performance of the random copolymers are greatly improved over those previously reported in the literature and indicate excellent promise as high temperature fuel cell membranes.

References

[1] B. C. H. Steele, A. Heinzel, *Nature* **2001**, *414*, 345.
[2] C. Yang, P. Costmagna, S. Srinivasan, J. Benziger, A. B. Bocarsly, *J. Power Sources* **2001**, *103*, 1.
[3] J. Mader, L. Xiao, T. Schmidt, B. C. Benicewicz, in *Advances in Polymer Science, Vol. 216* (Ed. G. Scherer), Springer-Verlag, Berlin, **2008**, pp. 63.
[4] J. S. Wainright, J. T. Wang, D. Weng, R. F. Savinell, M. Litt, *J. Electrochem. Soc*. **1995**, *142*, L121.
[5] D. Weng, J. S. Wainright, U. Landau, R. F. Savinell, *Proc.–Electrochem. Soc*. **1995**, *95*, 214.
[6] R. Savinell, E. Yeager, D. Tryk, U. Landau, J. Wainright, D. Weng, K. Lux, M. Litt, C. Rogers, *J. Electrochem. Soc*. **1994**, *141*, L46.
[7] Y. L. Ma, J. S. Wainright, M. H. Litt, R. F. Savinell, *J. Electrochem. Soc*. **2004**, *151*, A8.
[8] M. Kawahara, J. Morita, M. Rikukawa, K. Sanui, N. Ogata, *Electrochim. Acta* **2000**, *45*, 1395.
[9] M. Litt, R. Ameri, Y. Wang, R. Savinell, J. Wainright, *Mater. Res. Soc. Symp. Proc*. **1999**, *548*, 313.
[10] X. Glipa, B. Bonnet, B. Mula, D. J. Jones, J. Roziere, *J. Mater. Chem*. **1999**, *9*, 3045.
[11] M. K. Daletou, N. Gourdoupi, J. K. Kallitsis, *J. Membr. Sci*. **2005**, *252*, 115.
[12] V. Deimede, G. A. Voyiatzis, J. K. Kallitsis, Q. Li, N. J. Bjerrum, *Macromolecules* **2000**, *33*, 7609.
[13] C. Hasiotis, V. Deimede, C. Kontoyannis, *Electrochim. Acta* **2001**, *46*, 2401.
[14] J. Jeong, K. Yoon, J. Choi, Y. J. Kim, Y. T. Hong, *Membrein* **2006**, *16*, 276.
[15] J. A. Kerres, *J. Membr. Sci*. **2001**, *185*, 3.
[16] B. Kosmala, J. Schauer, *J. Appl. Polym. Sci*. **2002**, *85*, 1118.
[17] K. D. Kreuer, *J. Membr. Sci*. **2001**, *185*, 29.
[18] Q. Li, R. He, J. O. Jensen, N. J. Bjerrum, *Chem. Mater*. **2003**, *15*, 4896.
[19] C. Manea, M. Mulder, *Desalination* **2002**, *147*, 179.
[20] H. Pu, *Polym. Int*. **2003**, *52*, 1540.
[21] V. S. Silva, S. Weisshaar, R. Reissner, B. Ruffmann, S. Vetter, A. Mendes, L. M. Madeira, S. Nunes, *J. Power Sources* **2008**, *145*, 485.
[22] R. Wycisk, J. K. Lee, P. N. Pintauro, *J. Electrochem. Soc*. **2005**, *152*, A892.
[23] J. A. Asensio, S. Borros, P. Gomez-Romero, *J. Polym. Sci., Part A: Polym. Chem*. **2002**, *40*, 3703.
[24] P. Gomez-Romero, J. A. Asensio, S. Borros, *Electrochim. Acta* **2005**, *50*, 4715.
[25] J. A. Asensio, S. Borros, P. Gomez-Romero, *Electrochim. Acta* **2004**, *43*, 3821.
[26] J. M. Bae, I. Honma, M. Murata, T. Yamamoto, M. Rikukawa, N. Ogata, *Solid State Ionics* **2002**, *147*, 189.
[27] L. Xiao, H. Zhang, E. Scanlon, L. S. Ramanathan, E. W. Choe, D. Rogers, T. Apple, B. C. Benicewicz, *Chem. Mater*. **2005**, *17*, 5328.
[28] L. Xiao, H. Zhang, T. Jana, R. Chen, E. Scanlon, E. W. Choe, L. S. Ramanathan, S. Yu, B. C. Benicewicz, *Fuel Cells* **2005**, *5*, 287.
[29] S. Yu, B. C. Benicewicz, *Macromolecules* **2009**, *42*, 8640.
[30] G. Qian, B. C. Benicewicz, *J. Polym. Sci., Part A: Polym. Chem*. **2009**, *47*, 4064.
[31] G. Qian, D. W. Smith, B. C. Benicewicz, *Polymer* **2009**, *50*, 3911.
[32] S. Yu, H. Zhang, L. Xiao, E. W. Choe, B. C. Benicewicz, *Fuel Cells* **2009**, *9*, 318.
[33] J. A. Mader, B. C. Benicewicz, *Macromolecules* **2010**, *43*, 6706.
[34] H. Bai, W. S. W. Ho, *J. Taiwan Inst. Chem. Eng*. **2009**, *40*, 260.
[35] X. Glipa, M. El Haddad, D. J. Jones, J. Roziere, *Solid State Ionics* **1997**, *97*, 323.
[36] J. Peron, E. Ruiz, D. J. Jones, J. Roziere, *J. Membr. Sci*. **2008**, *314*, 247.
[37] M. J. Ariza, D. J. Jones, J. Roziere, *Desalination* **2002**, *147*, 183.
[38] Z. Bai, G. E. Price, M. Yoonessi, S. B. Juhl, M. F. Durstock, T. D. Dang, *J. Membr. Sci*. **2007**, *305*, 69.
[39] J. Jouanneau, R. Mercier, L. Gonon, G. Gebel, *Macromolecules* **2007**, *40*, 983.
[40] S. Qing, W. Huang, D. Yan, *Eur. Polym. J*. **2005**, *41*, 1589.
[41] M. Rikukawa, K. Sanui, *Prog. Polym. Sci*. **2000**, *25*, 1463.
[42] P. Staiti, F. Lufrano, A. S. Arico, E. Passalacqua, V. Antonucci, *J. Membr. Sci*. **2001**, *188*, 71.
[43] H. Xu, K. Chen, X. Guo, J. Fang, J. Yin, *Polymer* **2007**, *28*, 5556.
[44] D. J. Jones, J. Roziere, *J. Membr. Sci*. **2001**, *185*, 41.
[45] H. Bai, W. S. W. Ho, *Ind. Eng. Chem*. **2009**, *48*, 2344.
[46] H.-Y. Kim, J. W. Lee, T.-H. Lim, S. W. Nam, S.-A. Hong, I.-H. Oh, H. C. Ham, S.-Y. Lee, *US Patent, US 0241627A1*, **2008**.

